NONSUBSAMPLED HIGHER-DENSITY DISCRETE WAVELET TRANSFORM FOR IMAGE DENOISING

Arash Vosoughi, Azadeh Vosoughi, and Mohammad B. Shamsollahi

Sharif University of Technology, University of Rochester

ABSTRACT

Recently, a new set of dyadic wavelet frames based on oversampled filter banks is introduced that provides a higher sampling in both time and frequency, compared to the usual dyadic wavelets. This transform [1] (called HDDWT) is not *shift-invariant*; a feature which is desirable particularly for signal denoising. In this paper we propose a new transform, referred to as nonsubsampled HDDWT (NS-HDDWT), which is the shift-invariant version of HDDWT. The NS-HDDWT filter bank is built upon iterated nonsubsampled filter banks which are derived from the HDDWT filter bank in a way that is similar to the *a trous algorithm*. We employ HDDWT and NS-HDDWT for decomposition of images by performing the separable filtering. The performance of both HDDWT and NS-HDDWT is assessed in image denoising. Experimental results show that the performance of NS-HDDWT is superior to that of HDDWT, and in some cases NS-HDDWT outperforms powerful wavelet-based image denoising methods.

Index Terms— Wavelet transform, nonsubsampled filter bank, shift-invariant, image denoising.

1. INTRODUCTION

Images are usually contaminated by noise through their acquisition process. Additionally, noise can be introduced by transmission errors and compression. The aim of denoising techniques is to remove the noise from signal while retaining as much as possible the important signal features. In recent years, wavelet transforms have been emerged as the powerful tools for noise reduction applications [2]. Due to their useful properties, such as energy compaction and multiresolution structure, wavelet transforms enable a significant performance enhancement when applied for image denoising.

A wavelet frame is an expansive multiresolution transform that, in contrast to the critically sampled wavelet (DWT), provides a redundant representation for signals. The examples of such frames, which correspond to the oversampled filter banks, have been presented and used in noise reduction applications such as in [3], [4], [5], [6], and [7]. Such expansive transforms are usually preferred to the critically sampled DWT, particularly for noise removal purposes, due to following reasons: (1) they usually provide more than one detail subband which helps to better capture the signal features, (2) they can be nearly/completely shift-invariant, (3) more suitable filters can be designed by taking advantage of the more degrees of freedom generated by redundancy. Undecimated Discrete Wavelet Transform [2] (UDWT) is also an expansive multiresolution transform that has been extensively used in literature for image denoising. UDWT is associated to a nonsubsampled filter bank that is obtained from the DWT filter bank via the a trous algorithm [2]. Although UDWT is a completely shift-invariant transform, it has a two-channel filter bank that produces only one detail subband at each decomposition stage. Image denoising methods presented in [8] and [9] are among the best ones formulated in UDWT domain.

Recently, Selesnick developed an expansive dyadic wavelet frame that oversamples both time and frequency by a factor of two [1]. This new transform is implemented using oversampled digital filter banks and hence it is called Higher-Density Discrete Wavelet Transform (HDDWT). In this paper we first employ one dimensional HDDWT for decomposition of images by extending 1-D filtering to separable filtering. Then, we present the nonsubsampled HDDWT (NS-HDDWT), which is a shift-invariant version of the HDDWT. The NS-HDDWT is built upon iterated nonsubsampled filter banks that produce a shift-invariant multi-scale representation of signals. We use NS-HDDWT to decompose the images using the separable approach and show the effectiveness of the obtained 2-D NS-HDDWT in image denoising. The organization of this paper is as follows. In section 2 we describe how HDDWT filter bank can be used to decompose images. In section 3 we present the construction of the NS-HDDWT. In section 4, we present the experimental results that demonstrate the superior performance of NS-HDDWT to that of HDDWT, when they are applied to image denoising.

2. IMAGE DECOMPOSITION USING HDDWT

One dimensional HDDWT is implemented by the three channel filter bank illustrated in Fig. 1. H_0, H_1, and H_2 are low-pass, band-pass, and high-pass filters, respectively. The first two channels are down-sampled by two while the third channel is remained undecimated. We can adopt this expansive transform for decomposition of images via the

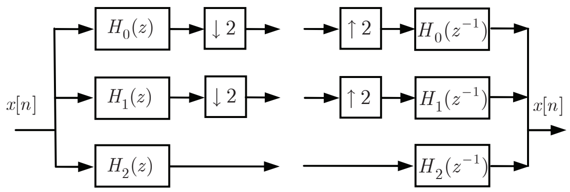

Fig. 1. The analysis and synthesis filter banks of higher-density discrete wavelet transform [1].

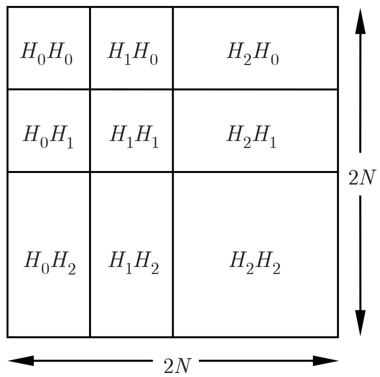

Fig. 2. Subband regions obtained by one-stage decomposition of an image whose size is $N \times N$.

separable implementation. To do this, the one dimensional HDDWT is first applied to all the rows of the image and then to all the resulted columns. Fig. 2 illustrates the subband regions obtained by one-stage decomposition of an $N \times N$ image. The subband located at the top left corner is approximation and the other eight subbands are details. The decomposition procedure can be iterated on the approximation subband correspondingly.

3. NONSUBSAMPLED HIGHER DENSITY DISCRETE WAVELET TRANFORM (NS-HDDWT)

HDDWT is not a shift-invariant transform, due to the down-samplers and up-samplers of its filter bank shown in Fig. 1. We propose a new filter bank based on the HDDWT filter bank which does not have the down/up-samplers and consequently is shift-invariant. The left part of Fig.3 illustrates two stages of decomposition using the proposed filter bank which we refer to as NS-HDDWT filter bank. The right part of this figure shows the synthesis part in which the input signal $x[n]$ is reconstructed from the outputs of the analysis part. The iterated NS-HDDWT filter bank is obtained from the HDDWT filter bank as follows: the down/up-samplers are removed, and the filters at each subsequent stage are up-sampled, such that the filters of j-th stage are obtained by up-sampling the filters of the first stage by a factor of 2^{j-1}. Such filter bank expansion is similar to the UDWT filter bank that is computed via the a trous algorithm. The three equivalent analysis filters of j-th stage of the NS-HDDWT filter bank are given by

$$H_{jk}^{eq}(z) = \begin{cases} \prod_{l=0}^{j-1} H_0(z^{2^l}), & k = 0 \\ H_1(z^{2^{j-1}}) \prod_{l=0}^{j-2} H_0(z^{2^l}), & k = 1 \\ H_2(z^{2^{j-1}}) \prod_{l=0}^{j-2} H_0(z^{2^l}), & k = 2 \end{cases} \tag{1}$$

where $H_{jk}^{eq}(z)$ represents the equivalent filter which includes filter $H_k(z^{2^{j-1}})$ at j-th stage of decomposition. Note that in NS-HDDWT synthesis filter bank the outputs of the channels are added up such that the outputs of the first two channels are equally weighted by 0.5, while the output of the third channel is not weighted. In the following we prove that the NS-HDDWT filter bank has the property of perfect reconstruction (PR) that is directly concluded from the fact that the HDDWT filter bank is PR.

Following [1], the perfect reconstruction conditions of HDDWT are

$$H_0(z)H_0(z^{-1}) + H_1(z)H_1(z^{-1}) + 2H_2(z)H_2(z^{-1}) = 2 \tag{2}$$

and

$$H_0(-z)H_0(z^{-1}) + H_1(-z)H_1(z^{-1}) = 0, \tag{3}$$

where H_0, H_1, and H_2 are the analysis filters of the HDDWT filter bank shown in Fig. 1. Now consider a NS-HDDWT filter bank which is constructed using the above filters and iteration through $j = 1, 2, \ldots, J$ stages. According to Fig. 3 and by doing some algebraic calculations, the perfect reconstruction condition of the analysis and synthesis filters at j-th stage is obtained as

$$\begin{aligned} &H_0(z^{2^{j-1}})H_0(z^{-2^{j-1}}) + H_1(z^{2^{j-1}})H_1(z^{-2^{j-1}}) + \\ &2H_2(z^{2^{j-1}})H_2(z^{-2^{j-1}}) = 2. \end{aligned} \tag{4}$$

The perfect reconstruction of the iterated NS-HDDWT filter bank is achieved conditioned that the filters of every stage build a PR filter bank, i.e., (4) is satisfied for $1 \le j \le J$. Note that if the filters H_0, H_1, and H_2 satisfy (2), they will also satisfy (4) for all values of j. This can be simply verified by changing the variable z in (2) to $z^{2^{j-1}}$. Thus, we conclude that if a HDDWT filter bank with the filter set H_0, H_1, and H_2 is PR, then its corresponding NS-HDDWT filter bank will be PR; since the filters satisfy PR condition of both of the filter banks simultaneously.

For a PR NS-HDDWT filter bank, the only condition to be satisfied is (4) or equivalently condition (2). Since unlike the HDDWT filter bank condition (3) is not required to be met, one can use the filter set of a HDDWT filter bank in a NS-HDDWT structure or can design new filters merely based on (2). The problem of designing novel filters for NS-HDDWT transform is under investigation and will be addressed in another paper.

The presented NS-HDDWT can be extended to multiple dimensions via the separable approach. For images there will be one approximation subband and eight detail

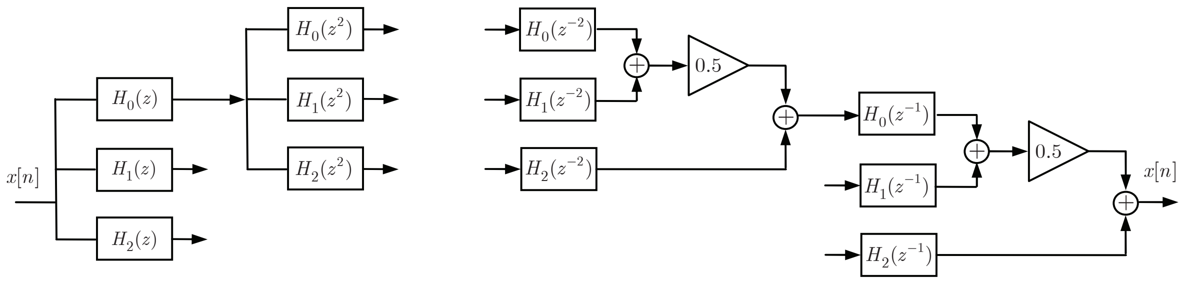

Fig. 3. The NS-HDDWT analysis and synthesis filter banks. Two stages of iteration are shown.

subbands at each stage of decomposition, each of them is the same size as the original image. Although NS-HDDWT is more redundant than HDDWT it has several advantages, compared to HDDWT, that justifies its application particularly in denoising. Primarily it is a fully shift-invariant transform which is a desirable feature in many applications especially in denoising [10]. Additionally the more redundancy of a representation helps to better estimate a signal from its noisy observation. Furthermore, note that NS-HDDWT can be implemented for arbitrary image sizes. This is in sharp contrast with HDDWT which can be only implemented for discrete signals or images whose sizes are a power of two, since the number of coefficients is halved in subsequent decomposition levels.

At the end of this section we briefly discuss that the presented NS-HDDWT filter bank underlies a tight frame expansion for signals in $l_2(\mathbb{Z})$. Following [11], a nonsubsampled filter bank implements a tight frame expansion if and only if its analysis filters are power complementary. To make the NS-HDDWT filter bank meet this condition, according to Fig. 3, we can change weight 0.5 to $2^{(-\frac{1}{2})}$ and give weight $2^{(-\frac{1}{2})}$ to the first two analysis filters. This change makes the analysis filters be power complementary, whereas the PR condition is being held.

4. EXPERIMENTAL RESULTS

In this section we attempt to remove additive white Gaussian noise (AWGN) from images via thresholding the 2-D NS-HDDWT coefficients of images. Following [12], we compute the threshold

$$T_S = \sigma_{nS}^2 / \sigma_S \tag{5}$$

for each detail subband S, where σ_{nS}^2 denotes the noise variance of S and σ_S is the standard deviation of noise free coefficients of S. To find σ_{nS}^2, the normalized noise variance of S and noise variance of the noisy image are estimated at first. The normalized noise variance of S is computed by averaging the variances of S for several normalized AWGN images. Noise variance of the noisy image can be estimated by the use of a robust estimator proposed in [13]. Then, σ_{nS}^2 is calculated by multiplication of the normalized noise variance of S and noise variance of noisy image. For every subband S, σ_S is estimated by

$$\sigma_S = \sqrt{\sigma_Y^2 - \sigma_{nS}^2}\,, \tag{6}$$

where σ_Y^2 is the variance of noisy coefficients of S. We locally apply soft thresholding on noisy coefficients, i.e., threshold (5) is estimated for each $W \times W$ sliding window in S. In our experiments we have used 13×13 non-overlapping sliding window for all the subbands. We have also applied this denoising scheme to 2-D HDDWT developed in section 2. We have compared our results with two of the best denoising techniques in the literature. The first one is the DWT-based bivariate shrinkage with local variance estimation [14]. The second one is Bayes least squares with a Gaussian scale-mixture model (BLS-GSM) [9] which is an excellent noise removal method formulated in UDWT domain. Table I illustrates the PSNR values obtained for the mentioned denoising algorithms. Results are obtained for different noise levels $\sigma_n =$ 10, 20, 30, 40, 50. According to this table we conclude that the performance of NS-HDDWT is superior to HDDWT in all the cases. Among the tested methods, NS-HDDWT yields the best results for the Barbara and Baboon images while BLS-GSM achieves better results for Lena image. We believe that NS-HDDWT will be able to perform more efficiently in image denoising provided that more effective estimators are employed. Note that BLS-GSM exploits a considerably more efficient and complex estimation than the simple thresholding estimation we have used for both NS-HDDWT and HDDWT. Fig. 4 shows the effect of the DWT-based and BLS-GSM denoising techniques on Barbara image corrupted by zero mean white Gaussian noise with $\sigma_n = 30$. In this figure a part of the image is zoomed-in in order to be able to compare the visual quality of the denoised images more accurately. According to these pictures we can see that NS-HDDWT and BLS-GSM remove the noise significantly while they yield considerably less ringing artifacts compared to the DWT-based method of bivariate shrinkage. Additionally, NS-HDDWT presents a better reconstruction than BLS-GSM. This can be observed by considering the linear structures of the pictures; in particular, the texture of the tablecloth is quite well recovered via NS-HDDWT thresholding, though, it is slightly destructed (blurred) when the BLS-GSM is used.

Table I. Average PSNR values of denoised images over five runs of different denoising methods on various test images. For both HDDWT and NS-HDDWT, the filter set of example 3 designed in [1] is used.

Barbara	PSNR (dB)				
σ	Noisy	Biv-Shrink	BLS-GSM	HDDWT	NS-HDDWT
10	28.16	32.16	33.42	32.95	**33.49**
20	22.15	28.26	29.42	29.09	**29.66**
30	18.63	26.17	27.08	26.93	**27.49**
40	16.13	24.83	25.59	25.55	**26.11**
50	14.18	23.89	24.53	24.52	**25.02**

Lena	PSNR (dB)				
σ	Noisy	Biv-Shrink	BLS-GSM	HDDWT	NS-HDDWT
10	28.16	34.35	**35.41**	34.76	35.20
20	22.16	31.17	**32.38**	31.53	32.12
30	18.62	29.38	**30.55**	29.67	30.26
40	16.15	28.16	**29.26**	28.36	28.97
50	14.18	27.12	**28.21**	27.34	27.85

Baboon	PSNR (dB)				
σ	Noisy	Biv-Shrink	BLS-GSM	HDDWT	NS-HDDWT
10	28.16	28.64	30.40	30.25	**30.51**
20	22.14	25.29	26.26	26.17	**26.46**
30	18.64	23.39	24.12	24.11	**24.44**
40	16.12	22.23	22.88	22.83	**23.18**
50	14.20	21.44	22.02	21.98	**22.28**

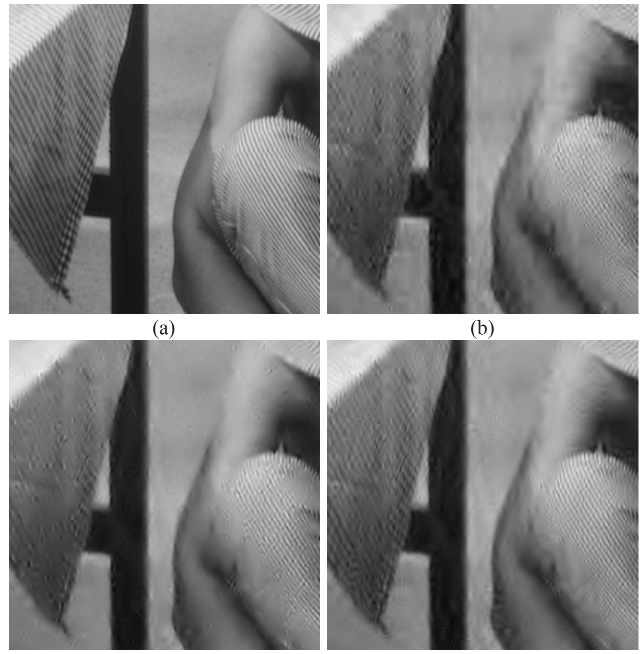

(a) (b) (c) (d)

Fig. 4. (a) Original "Barbara" image. The noise intensity is 30. (b) Denoised with DWT-based bivariate shrinkage [14], PSNR = 26.17. (c) Denoised with BLS-GSM [9], PSNR = 27.08. (d) Denoised via local thresholding in NS-HDDWT domain, PSNR = 27.49.

5. CONCLUSION

We have proposed the new transform of nonsubsampled higher-density discrete wavelet transform which is the shift-invariant version of the HDDWT. We have used NS-HDDWT for image denoising by performing local thresholding of the 2-D NS-HDDWT coefficients of images. Our preliminary results are promising and they show that NS-HDDWT performs better than HDDWT and has comparable performance to powerful wavelet-based denoising methods. We expect that the performance of NS-HDDWT can be greatly enhanced if the simple thresholding approach is substituted with a more sophisticated estimation method.

6. REFERENCES

[1] I. W. Selesnick, "A higher-density discrete wavelet transform," *IEEE Trans. on Signal Processing*, vol. 54, no. 8, pp. 3039-3048, Aug. 2006.

[2] S. Mallat, *A Wavelet Tour of Signal Processing*, 2nd Ed. Academic, New York, 1999.

[3] Z. Cvetkovic´ and M. Vetterli, "Overcomplete expansions and robustness," in *Proc. IEEE Int. Symp. Time-Frequency Time-Scale Analysis*, pp. 325–328, 1996.

[4] L. Rebollo-Neira, A. G. Constantinides, and T. Stathaki, "Signal representation for compression and noise reduction through frame-based wavelets," *IEEE Trans. on Signal Processing*, vol. 46, no. 3, pp. 587–597, Mar. 1998.

[5] I.W. Selesnick and L. Sendur, "Smooth wavelet frames with application to denoising," in *Proc. IEEE Int. Conf. Acoust., Speech, Signal Process.*, vol. 1, pp. 129–132, June 2000.

[6] A. F. Abdelnour and I. W. Selesnick, "Symmetric nearly shift-invariant tight frame wavelets," *IEEE Trans. on Signal Processing*, vol. 53, no. 1, pp. 231- 239, Jan 2005.

[7] A. F. Abdelnour, "Dual-Tree tight frame wavelets with symmetric envelope," in *Proc. IEEE Int. Conf. ICTTA*, pp. 1–6, April 2008.

[8] S. G. Chang, B. Yu, and M. Vetterli, "Spatially adaptive wavelet thresholding with context modeling for image denoising" *IEEE Trans. on Image Processing*, vol. 9, no. 9, pp. 1522-1531, Sept. 2000.

[9] J. Portilla, V. Strela, M. J. Wainwright, and E. P. Simoncelli, "Image denoising using scale mixtures of Gaussians in the wavelet domain," *IEEE Trans. on Image Processing*, vol. 12, no. 11, pp. 1338-1351, Nov. 2003.

[10] R. R. Coifman and D. L. Donoho, "Translation-invariant denoising," in *Wavelets and Statistics*, A. Antoniadis and G. Oppenheim, Eds. Berlin, Germany: Springer-Verlag, 1995.

[11] Z. Cvetkovic´ and M. Vetterli, "Oversampled filter banks," *IEEE Trans. on Signal Processing*, vol. 46, no, 5, pp. 1245-1255, May 1998.

[12] S. Chang, B. Yu, and M. Vetterli, "Adaptive wavelet thresholding for image denoising and compression," *IEEE Trans. on Image Processing*, vol. 9, no. 9, pp. 1532–1546, Sept. 2000.

[13] D. L. Donoho and I. M. Johnston, "Ideal spatial adaptation via wavelet shrinkage," *Biometrika*, vol. 81, pp. 425–455, 1994.

[14] L.Sendur and I. W. Selesnick, "Bivariate shrinkage with local variance estimation," *IEEE Signal Processing Letter*, vol. 9, no. 12, pp. 438-441, Dec. 2002.